Solid-State High-Resolution Carbon-13 NMR Studies of Celluloses

AUTHOR(S):

Hirai, Asako; Horii, Fumitaka; Kitamaru, Ryozo

Bull. Inst. Chem. Res., Kyoto Univ., Vol. 63, No. 4, 1985

REVIEW

Solid-State High-Resolution Carbon-13 NMR Studies of Celluloses

Asako HIRAI, Fumitaka HORII and Ryozo KITAMARU

Received November 14, 1985

KEY WORDS: CP/MAS ^{13}C NMR/ Celluloses/ Crystalline and non-crystalline components/ Molecular chain conformation/ MAS rotor with an O-ring seal

INTRODUCTION

The solid-state high resolution ^{13}C NMR provides an insight into the conformation and dynamics of molecular chains *via* chemical shift and magnetic relaxation. This paper reviews briefly its basic principle and recent application to different celluloses including cotton, ramie, bacterial, valonia, and regenerated celluloses.

NUCLEAR MAGNETIC RESONANCE IN SOLIDS

The Hamiltonian of a spin system in a static field B_0 mainly consists of (1) the direct interaction H_Z of spins with B_0 (2) the indirect interaction H_S of spins with B_0 *via* electrons and (3) the dipole-dipole interaction H_D among spins.

$$H=H_Z+H_S+H_D \qquad (1)$$

The H_Z, the so-called Zeeman energy, gives zero'th order absorption lines (one to each nuclear species). The H_D gives the linewidth to the zero'th order lines whereas the H_S gives different shifts depending on the local electronic environment around nuclei. In the high resolution NMR in solution, the chemical shifts due to the H_S are observed. In solids, however, no absorption line reflecting the contribution of H_S is usually recognizable because of the line broadening by H_D. Accordingly, the first step to obtain a high resolution spectrum in the solid state is to eliminate the contribution of H_D. In ^{13}C NMR on substances containing only ^{13}C and ^{1}H as spin-having nuclei, this can be easily done in principle by applying an oscillating magnetic resonance field on ^{1}H. The dipolar interaction between ^{13}C and ^{1}H is averaged to zero with the rapid direction change of ^{1}H spin by this technique which is called "^{1}H dipolar decoupling (DD)". Since ^{13}C-^{13}C dipolar interaction is negligible because of very low natural abundance of the nucleus, the spectrum contributed from H_S is actually observable by this technique even for solid matter.

* 平井諒子, 堀井文敬, 北丸竜三 : Laboratory of Fiber Chemistry, Institute for Chemical Research, Kyoto University, Uji, Kyoto 611.

However, all conditions necessary for obtaining a high resolution spectrum are not yet fulfilled. This is obvious from the explicit form of H_S produced by the spin I with B_0

$$H_S=\hbar I\cdot\sigma B_0 \text{ with } \hbar=h/2\pi \qquad (2)$$

Here, σB_0 represents the shielding magnetic field induced by electrons against B_0. σ is the second rank tensor which operates on B_0 and produces σB_0 as a vector. Therefore, even if H_D is removed, the spectrum is not observable as a sharp line.

The σ definable for the carbon in each molecular conformation is generally characterized by three principal values in the principal axis frame. Hence, the contribution to the spectrum from a given carbon species depends on the molecular conformation to which the carbon belongs. In the case of a powder crystal, for example, a characteristic spectrum is determined by three principal values σ_{11}, σ_{22}, and σ_{33}. In a particular case that the σ_{33} axis coincides with molecular chain axis such as in polyethylene[1-3] and poly(ethylene terephthalate)[3] a sharp line corresponding to σ_{33} is actually observed, provided the measurement is conducted for oriented samples with the fiber axis parallel to B_0. In fact, the detailed phase structure of a well-oriented linear polyethylene has been elucidated by ^{13}C NMR with use of this DD technique.[2]

For general macromolecules containing many carbon species, the spectrum obtained only with DD is generally unresolvable because of the superposition of the contributions from different carbon species. Then, the technique which is called "magic angle sample spinning (MAS)" becomes unavoidable. This is a technique that samples are rotated around an axis which makes an angle of 54°44' to B_0. Since, the angle 54°44' corresponds to the angle between the diagonal and each side of a cube, such spinning provides equal averaging of the principal values of σ in relation to three principal axes. Then, by sufficiently rapid spinning, a sharp line can be observed at the average σ for each carbon.

In the solid-state ^{13}C NMR, there is another widely used technique in addition to the above-mentioned techniques. It is a technique to enhance the ^{13}C magnetization through the energy exchange between ^{13}C and ^{1}H nuclei, which is called "cross-polarization (CP)" or "proton enhancement". In order to observe the magnetization of the rare ^{13}C, this technique is often very effective. However, it is not always indispensable in principle, though the solid-state NMR would not have been developed rapidly without this technique. Furthermore, it should be noted that the CP efficiency frequently depends on the carbon species as well as the state of samples.

MAGNETIC RELAXATION

As mentioned above, high resolution spectra are obtainable for solids by combining DD, MAS and CP. Then, one can inquire the chain conformation in both crystalline and noncrystalline states of macromolecules in terms of chemical shifts. Moreover, if the magnetic relaxation is simultaneously measured, more detailed information about the molecular chain conformation and dynamics is expected.[4] This section introduces the outline of the magnetic relaxation.

A spin system generally produces a magnetization in the direction of B_0 as a result of the equilibrium with other degrees of freedom such as the rotation and vibration of atoms and molecules; these degrees of freedom are usually called "lattice". When the magnetization is deviated from the equilibrium value, it returns to the equilibrium value. This process is the "magnetic relaxation". The relaxations in the directions parallel and perpendicular to B_0 are widely measured; the former is called "spin-lattice relaxation (or logitudinal relaxation)" because it accompanies the energy exchange between the spin system and the lattice, and the latter "spin-spin relaxation (or transverse relaxation)" because it is carried out by the spin exchange within the spin system. Let a rectangular coordinate be (x, y, z) with z- axis parallel to B_0, and M_z and M_x be the magnetizations in z and x-directions. Then these relaxations are generally described as a function of time lapse t:

$$M_z(t)-M_z^0=[M_z(0)-M_z^0]\exp(-t/T_1) \tag{3}$$

$$M_x(t)=M_x(0)\ \exp(-t/T_2) \tag{4}$$

Here, M_z^0 denotes the equilibrium magnetization. The time constants T_1 and T_2 characterize the longitudinal and transverse relaxations, respectively.

In addition to these relaxations, there are many relaxations such as nuclear Overhauser enhancement and longitudinal relaxation in the rotating frame, but this paper deals only with the longitudinal and transverse relaxations. These relaxations are generally conducted by the mutual transitions among zero'th order eigenstates of the spin system. Hence, any mechanism that initiates the perturbation of magnetic field including the frequency components that correspond to the energy differences among zero'th order eigenstates induces the above-mentioned magnetic relaxations. In the case of macromolecules, it is well established that the relaxations of ^{13}C magnetization are predominantly carried out by time-fluctuating H_D between chemically bonded ^{13}C and ^{1}H. If the spectral densities $J_m(\omega)$ are defined to be Fourier transforms of the time correlation functions of the orientation functions that characterize the orientation of the internuclear C-H vector, T_1 and T_2 are described as

$$1/T_1=(1/20)\gamma_H^2\gamma_C^2\hbar^2r^{-6}[J_0(\omega_H-\omega_C)+3J_1(\omega_C)+6J_2(\omega_H+\omega_C)] \tag{5}$$

$$1/T_2=(1/40)\gamma_H^2\gamma_C^2\hbar^2r^{-6}[4J_0(0)+J_0(\omega_H-\omega_C)+3J_1(\omega_C)+6J_1(\omega_H)+6J_2(\omega_H+\omega_C)] \tag{6}$$

Here, γ_H and γ_C, and ω_H and ω_C are the magnetogyric ratios and Larmor frequencies of ^{1}H and ^{13}C, respectively. r denotes the internuclear distance. $J_m(\omega)$ depend on the motional mode of the C-H vector. In the case, for example, that it undergoes the spherical diffusional rotation with a correlation time τ_c, the correlation functions of the orientation functions $Y_m(t)$ of the C-H vector are described in the forms of $|Y_m(0)|^2\exp(-t/\tau_c)$. Hence, the spectral densities $J_m(\omega)$ become to

$$J_m(\tau)=2\tau_c/(1+\omega^2\tau_c^2) \tag{7}$$

If it is assumed that $B_0=2.35$ T ($\omega_H=6.28\times10^8$ Hz, $\omega_C=1.57\times10^8$ Hz), T_1 should be determined by the motion of the C-H vector in a frequency range of about 10^8 Hz.

On the other hand, it is noted that T_2 is related to much slower molecular motion than that related to T_1 since it contains the contribution of the motion of $\omega=0$ as is revealed from eq. (6).

SOLID STRUCTURE OF CELLULOSE

Cellulose molecules contain six kinds of carbon species as shown in Fig. 1. The ^{13}C NMR spectrum without magic angle sample spinning is unresolved for individual carbons. However, the magic-angle sample spinning process enables to resolve the absorption signals for most of the individual carbons as shown below. Furthermore, since the molecular chains are fairly rigid, the rate of cross-polarization

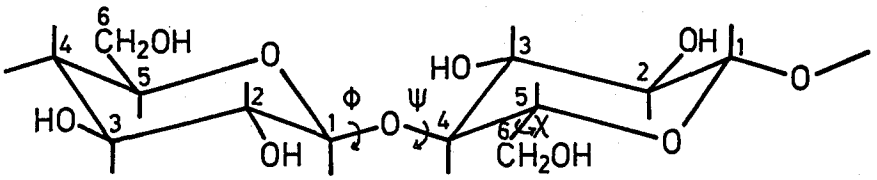

Fig. 1. Chemical structure of cellulose and the definition of three torsion angles.

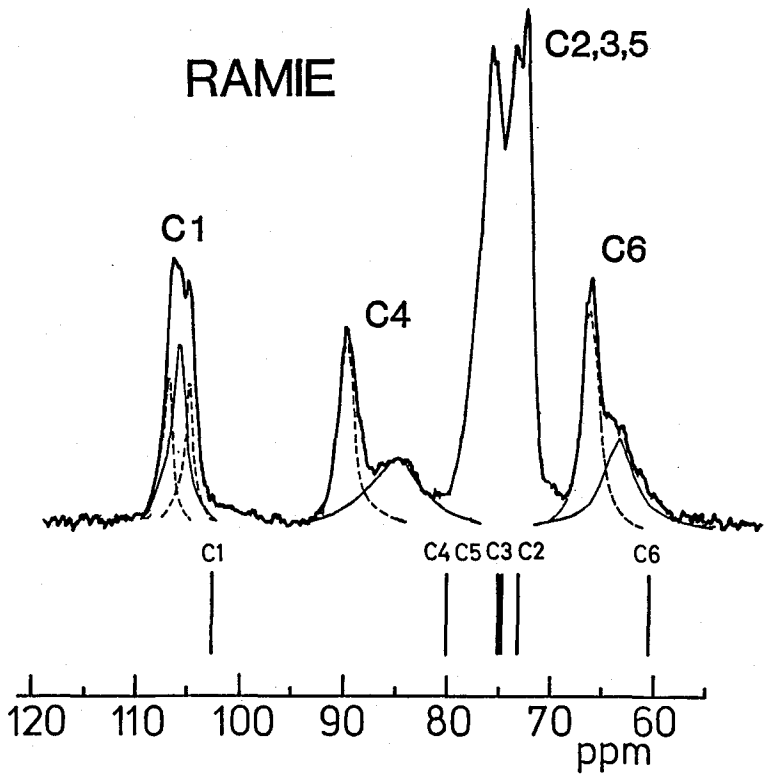

Fig. 2. 50 MHz CP/MAS ^{13}C NMR spectrum of ramie and stick-type scalar-decoupled ^{13}C NMR spectrum of low-molecular-weight cellulose in DMSO-d_6 solution. Broken and thin solid lines in the CP/MAS spectrum are the crystalline and noncrystalline components, respectively.

is almost equivalent for the crystalline and noncrystalline states for all carbon species.[5] The CP process can be efficiently used in most cases of studies.

a. Assignments of Absorption Lines of Individual Carbons in the Crystalline and Noncrystalline Regions[6]

Figure 2, shows a CP/MAS ^{13}C NMR spectrum of well-dried ramie cellulose with a stick-type spectrum of low molecular weight cellulose[7] (DP$\sim$10) in deuterated dimethyl sulfoxide solution. The signals of C1, C4 and C6, concerning the β-1,4-glycosidic linkage and the exo-cyclic C5-C6 bond, can be well assigned as reported[8,9] while the signals for C2, C3 and C5 are not resolved so well. It can be seen that the resonance lines of C1, C4 and C6 are shifted downfield by 2.3–9.6 ppm in comparison with those of the low molecular weight cellulose in solution. The cause of such downfield shifts is mainly attributed to the intrinsic chain conformation in the solid state as discussed later. In addition, the lines of the C4 and C6 split into two components; sharp downfield and broad upfield components. Similar splittings are observed also for the C4 and C6 resonance lines of cotton, bacterial and valonia celluloses, and regenerated celluloses such as cupra rayon. In relation to the C4 lines, it was noted for samples with different crystallinities over a wide range that the downfield intensity decreases and the upfield intensity increases with decreasing crystallinity of samples. Then an assumption was made that the sharp downfield and broad upfield signals were contributed from the crystalline and noncrystalline components, respectively.[10] We have decomposed the C4 signals into two Lorentzian downfield and upfield com-

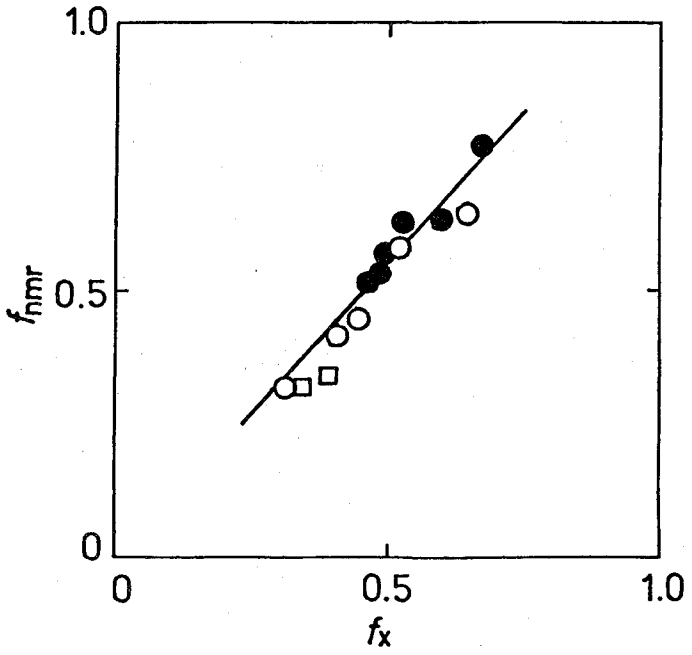

Fig. 3. Integrated fraction f_{nmr} of the downfield component of the C4 resonance line vs. degree of crystallinity f_x determined by x-ray analysis. ●: native cellulose, ○: regenerated cellulose, □: mercerized cotton and ramie.

ponents for different cellulose samples with different crystallinities in order to confirm this assumption. In Fig. 3, the integrated intensity of the downfield component is plotted against the degree of crystallinity estimated from *x*-ray analyses. It is evident that a linear relationship exists between the integrated fraction of the downfield component and the degree of crystallinity. A similar result was obtained for the C6 signals. It is then concluded that the sharp downfield and broad upfield components of the C4 and C6 carbons of different cellulose samples, including native and regenerated celluloses, are contributed from the crystalline and noncrystalline components, respectively.

b. Crystalline and Noncrystalline Spectra of Various Cellulose Samples

As mentioned above, the signals of C4 and C6 carbons consist of the downfield crystalline and upfield noncrystalline components. Hence, the signals of all carbon species are thought to consist of the crystalline and noncrystalline components even if they cannot be seen explicitly in the spectra. If the ^{13}C spin-lattice relaxation times are sufficiently different between the crystalline and noncrystalline lines for all carbon species, the crystalline and noncrystalline spectra can be recorded separately using the difference in T_1 as mentioned below.

Table 1 summarizes the T_1's of some samples,[5] which were obtained by Torchia's pulse sequence shown in Fig. 4.[11] It is seen that for all samples examined each carbon contains distinctly different (long and short) two T_1's, although the shorter T_1 of bacterial cellulose could not be discerned except for C2, C3, C5 because of the high crystallinity. The longer and shorter T_1's for each carbon are assignable to the crystalline and noncrystalline components, respectively. The comparison of the longer and shorter T_1's among the samples provides some information of the molecular chain mobility of both crystalline and noncrystalline components.[5] However, we attempt here only to obtain separately the crystalline and noncrystalline spectra by use of the difference in T_1.

Figure 5 shows the crystalline spectrum of dry cotton cellulose obtained by the pulse sequence shown in Fig. 4, where the delay time τ between the two ^{13}C $\pi/2$ pulses was 100 s. Although the relative line intensities of different carbon species are not quantitatively valid because of the difference in T_1's of individual carbons, the chemical shifts and linewidths of C1, C4 and C6 could be determined accurately, eliminating the noncrystalline contributions. (Figure 6 shows the similar crystalline spectra of other native cellulose samples in the dry state.) In Table 2, the chemical

Table 1. ^{13}C Spin-Lattice Relaxation Times of the Carbons of Different Cellulose Samples Measured at 25 MHz.

Sample	T_1/s							
	C1		C4		C6		C2, 3, 5	
ramie	76	8.8	130	16	65	4.6	82	8.3
cotton	78	~7	87	11	89	~7	67	~8
bacterial	87	—	107	—	86	—	104	5.7
cupra rayon	58	6.8	82	9.9	53	4.2	37	4.7

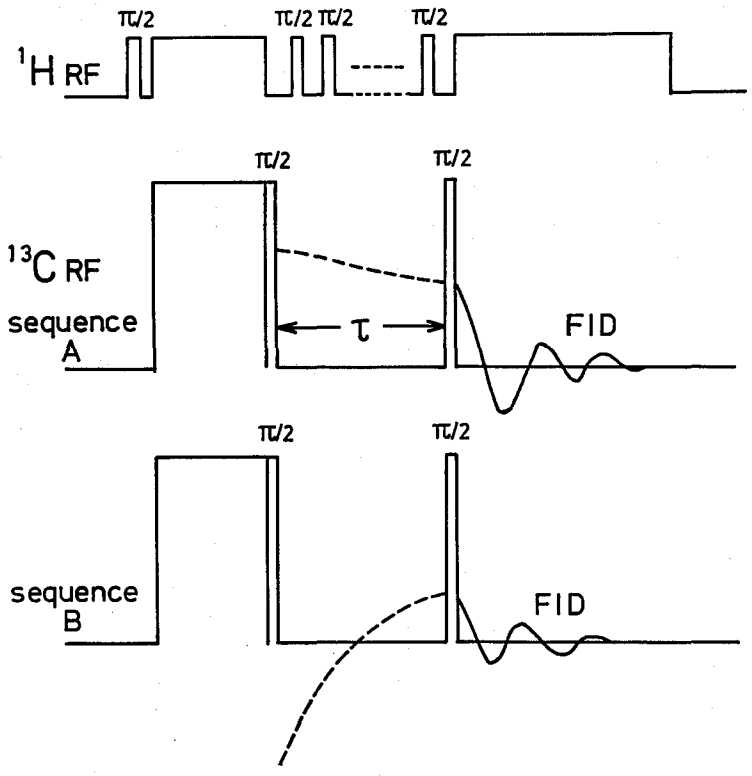

Fig. 4. Pulse sequence employed for the measurement of ^{13}C spin-lattice relaxation time T_1.

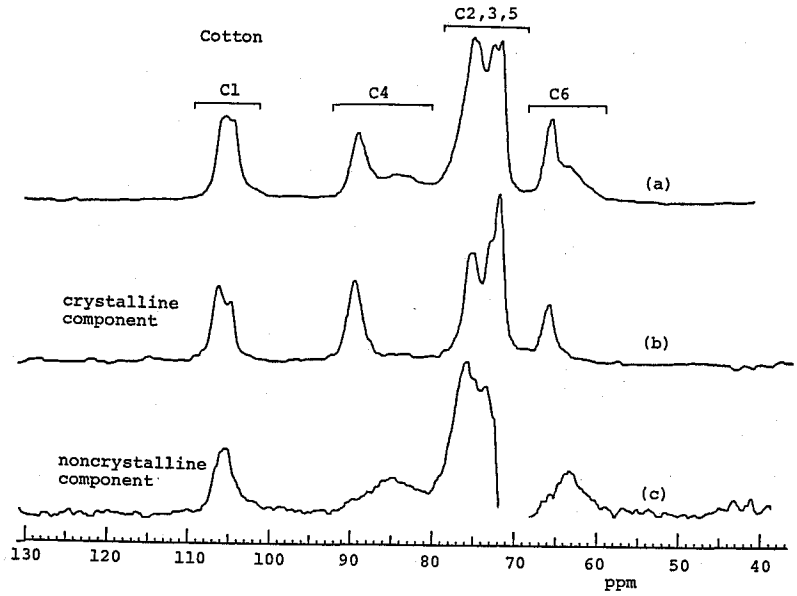

Fig. 5. 50 MHz CP/MAS ^{13}C NMR spectra of cotton. (a) whole spectrum; (b) crystalline component; (c) noncrystalline component.

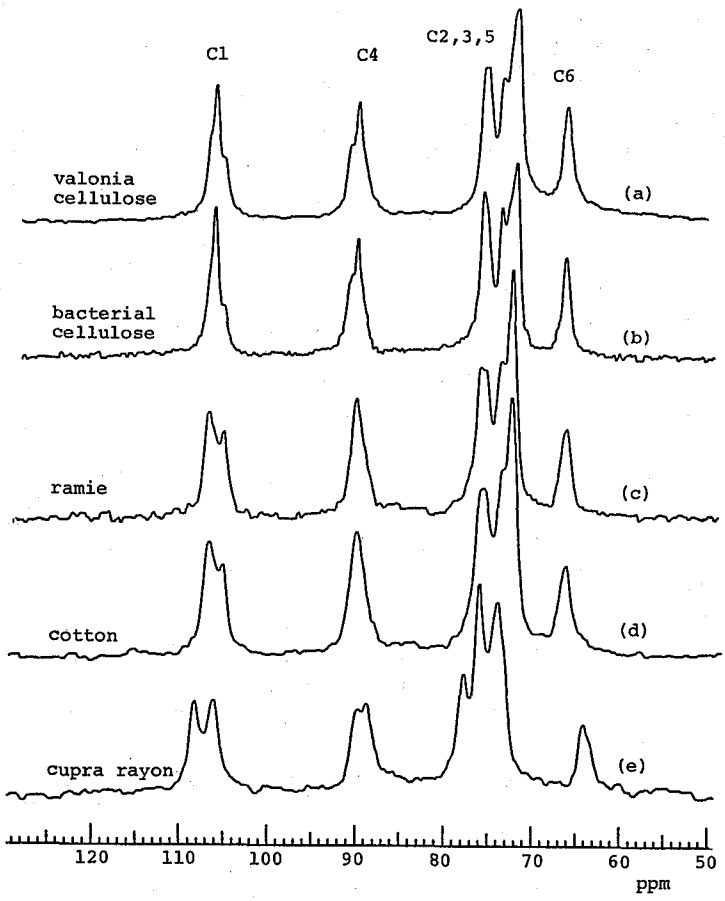

Fig. 6. CP/MAS ^{13}C NMR spectra of the crystalline components of dry cellulose samples. (a) valonia cellulose, (b) bacterial cellulose, (c) ramie, (d) cotton, (e) cupra rayon.

Table 2. ^{13}C Chemical Shifts of the Crystalline Components of Native and Regenerated Celluloses

sample	chemical shift/ppm					
	C1			C4		C6
native cellulose						
valonia	107.0	106.4	105.3	91.3	90.1	66.5
bacterial	107.3	106.3	105.3	91.0	90.1	66.4
ramie	107.0		105.2	90.0		66.2
cotton	107.1		105.4	89.9		66.5
regenerated cellulose						
cupra rayon	108.0		106.3	89.5	88.2	64.1
high-crystalline cellulose II	108.1		106.3	89.6	88.4	63.7

shifts obtained from such crystalline spectra on native and regenerated cellulose samples are filed. We will consider later these data in relation to the molecular chain conformation of the crystalline component of the samples.

On the other hand, the noncrystalline spectra can be obtained by subtracting adequately the crystalline spectrum from the corresponding whole spectrum including both crystalline and noncrystalline contributions. An example is given in Fig. 5c, where the noncrystalline spectrum of cotton obtained by the subtraction of Fig. 5b from Fig. 5a. The chemical shifts and linewidths of C1, C4 and C6 estimated from such noncrystalline spectra of different samples are listed in Table 3. These data will be also discussed later in relation to the chain conformation of the noncrystalline component.

Table 3. ^{13}C Chemical Shifts and Line-Widths of the Noncrystalline Components of Native and Regenerated Celluloses

sample	C1		C4		C6	
	δ/ppm	$\Delta\nu$/Hz	δ/ppm	$\Delta\nu$/Hz	δ/ppm	$\Delta\nu$/Hz
native cellulose						
valonia	106.2	114	85.2	249	63.4	185
bacterial	106.6	120	85.0	242	63.4	163
ramie	105.8	128	84.8	284	63.0	171
cotton	106.0	143	85.1	256	63.7	185
regenerated cellulose						
cupra rayon	105.3	284	85.1	327	62.8	185

c. Molecular Chain Conformation and Chemical Shifts of C1, C4, C6 Carbons

The chemical shift observed by CP/MAS NMR technique is the average value (σ_{av}) of the principal values of the chemical shift tensor. This chemical shift (σ_{av}) reflects of course the electronic environment around the nucleus concerned. The electronic environment is thought to depend on the packing state of molecules and the hydrogen bonding as well as the molecular chain conformation. Only a little is known about the relationship between the chemical shifts and these parameters for different substances at present. In relation to the packing effect, for example, VanderHart[12] has found that the resonance line of central CH_2 carbons of triclinic crystals of n-$C_{20}H_{42}$ is shifted 1.3 ± 0.4 ppm downfield in comparison to that of n-paraffins of other crystal forms. As for the hydrogen bonding effect, Terao et al.[13,14] have reported that large downfield shifts appear for the carbons bonded chemically to hydroxyl groups which form strong hydrogen bonds. First, we have examined these two effects for the crystals of monosaccharides and disaccharides which are low-molecular compounds related to cellulose.[6]

Table 4 compares the ^{13}C CP/MAS chemical shifts of these components in the crystalline state and in the D_2O solution. The comparison is made only for carbons which are not associated with the exo-cyclic C-C bonds and β-1,4-glycosidic linkages. The respective resonance lines of the solid-state spectra on α- and β-glucoses and those of the solution spectra of all samples were assigned according to the results of Pfeffer

Table 4. Comparison of ^{13}C Chemical Shifts of Monosaccharides and Disaccharides in the Solid State and in Solution

Sample	Carbon	δ/ppm		Δδ/ppm	O···O distance/A
		Solid	D_2O solution		
α-D-glucose	1	93.54	93.30	0.24	2.847
	2	71.22	72.73	−1.51	2.776
	3	73.75	74.05	−0.30	2.707
	4	73.36	70.93	2.43	2.773
β-D-glucose	1	97.34	97.15	0.19	2.666
	2	76.39	75.46	0.93	2.686, 2.708
	3	76.39	77.17	−0.78	2.772
	4	70.34	70.93	−0.59	no
β-D-cellobiose	1′	98.02	97.05	0.97	2.776
α-D-lactose monohydrate	1′	93.50	93.15	0.35	2.790
β-D-lactose	1′	99.00	97.10	1.90	2.772

et al.[15,16] In the table, the O···O distances of the hydrogen bonds in the solid state are also shown. The difference Δδ in chemical shift between in the solid and solution ranges from −1.51 ppm to 2.43 ppm. Nevertheless, it is difficult to find any dependency of the chemical shifts on the O···O distances. It is then concluded that the hydrogen bonding does not significantly affect the chemical shifts in these carbo-

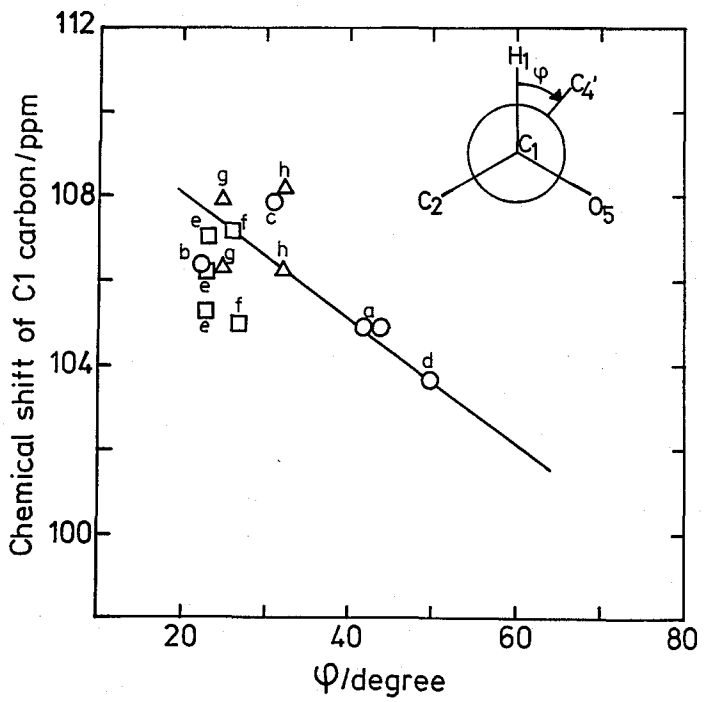

Fig. 7. ^{13}C chemical shifts of the C1 carbons vs. torsion angles ϕ. a: β-D-cellobiose, b: β-D-methyl cellobioside·CH_3OH, c: α-D-lactose monohydrate, d: β-D-lactose, e: cellulose I, f: cellulose I, g: cellulose II, h: cellulose II.

hydrates as well as in cellulose. However, downfield or upfield shifts less than about 2.5 ppm may be produced as a result of the combined intermolecular effect of the packing and hydrogen bonding.

Next, we have examined the relationship between the chemical shift and the molecular chain conformation. The chain conformation of cellulose molecules is defined in terms of three torsion angles as shown in Fig. 1[6]; ϕ and ψ around the β-1,4-glycosidic linkages and χ around the C5-C6 bonds. In order to find out the relationships between the chemical shifts and the torsion angles in cellulose samples, the chemical shifts of different disaccharides with β-1,4-glycosidic linkages were examined, the torsion angles of which are known from x-ray diffraction analyses.[17-21] In Fig. 7, the chemical shifts of the C1 carbon of the different disaccharides are plotted against the torsion angle ϕ. The chemical shifts of the crystalline C1 carbon of cellulose samples which are shown in Table 2 are also plotted in the figure using the ϕ values reported.[22-25] In such cases that two or three different chemical shifts are observed and only one ϕ is reported, all chemical shifts are plotted against the same ϕ. Although the data are somewhat scattered possibly because of the intermolecular effect, the C1 chemical shift seems to be correlated to the torsion angle ϕ.

The similar plots of the C4 and C6 chemical shifts against the torsion angles ψ and

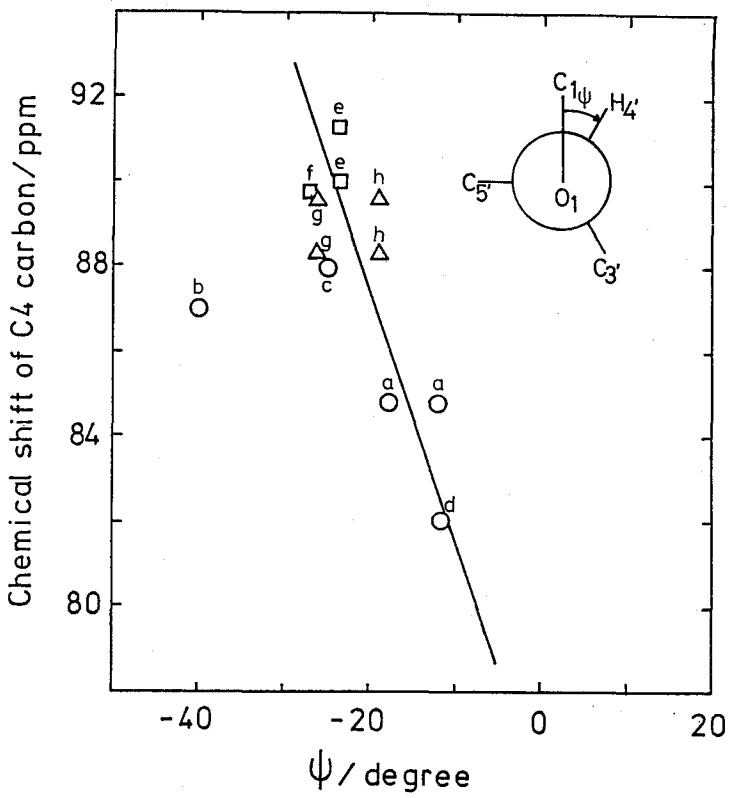

Fig. 8. ^{13}C chemical shifts of the C4 carbons vs. torsion angles ψ. a: β-D-cellobiose, b: β-D-methyl cellobioside·CH_3OH, c: α-D-lactose monohydrate, d: β-D-lactose, e: cellulose I, f: cellulose I, g: cellulose II, h: cellulose II.

χ obtained from *x*-ray analyses are shown in Figs. 8 and 9.[6] It is evident that the C4 and C6 chemical shifts depend primarily on these torsion angles, ψ and χ, respectively. According to a recent survey[26] of the rotation about the C5-C6 bonds in low molecular weight glucosides, *gauche-gauche* and *gauche-trans** are the two favorable conformers. In agreement with this survey, no data of monosaccharides and disaccharides are included in Fig. 9 which correspond to the χ of ca. 300° (*trans-gauche*). On the other hand, the conformation of the CH_2OH side groups of the crystalline component of native cellulose is found to be *trans-gauche*[22,24] against the expectation from the data of monomeric glucosides. It is found from Fig. 9 that three preferred conformation, *gauche-gauche*, *gauche-trans*, and *trans-gauche* correspond to the chemical shifts of about 62, 62.7–64.5, and 66 ppm, respectively.[27]

It is concluded that the solid-state chemical shifts of the C1, C4, and C6 carbons

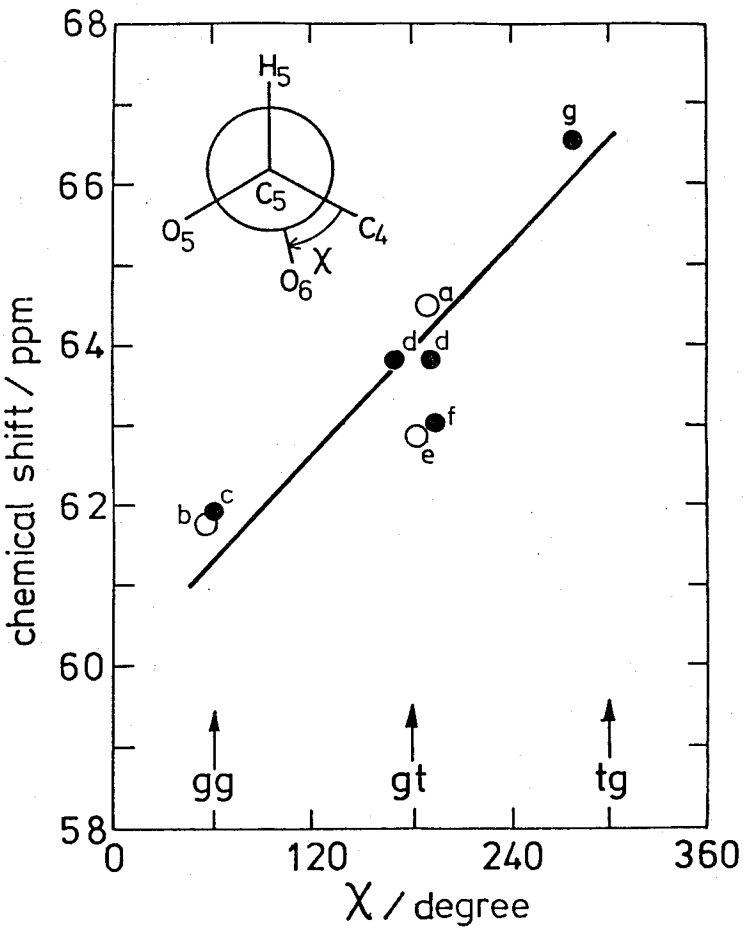

Fig. 9. ^{13}C chemical shifts of the C6 carbons vs. torsion angles χ. a: α-D-glucose, b: α-D-glucose monohydrate, c: β-D-glucose, d: β-D-cellobiose, e: α-D-lactose monohydrate, f: β-D-lactose, g: cellulose I.

* The C6-O6 bond is *gauche* in relation to bond O5-C5 and *trans* in relation to bond C4-C5.

are mainly correlated to the torsion angles ϕ, ψ, and χ, respectively. However, the intermolecular effects such as packing and hydrogen bonding produce totally the downfield or upfield shift of 0.2–2.4 ppm for the carbohydrates studied here. Therefore, when the downfield or upfield shift of such an order appears even in the solid-state ^{13}C NMR spectra, the intermolecular effects must be also considered.

Now, we are in a situation to be able to discuss the crystalline and noncrystalline chemical shifts for different cellulose samples. First consider the chemical shifts of the crystalline components shown in Table 2. The C1 resonance lines of native cellulose seem to split into two or three lines, although the relative intensities of the doublet of cotton and ramie are greatly different from those of bacterial and valonia celluloses (as clearly seen in Fig. 6). In addition, the C4 lines in the latter celluloses split into the upfield main line and the downfield shoulder. If these splittings are associated with the different torsion angles in the β-1,4-glycosidic linkages, the splitting of 1.0–1.6 ppm recognized in the C1 carbon and that of 0.7–0.9 ppm in C4 carbon correspond to the differences of 6.7–10.7° and 1.2–1.5° in the torsion angles ϕ and ψ, respectively (ref. Figs. 7, 8).

An alternative cause of the splittings may be the intermolecular effect because the extent of splittings are in the order of the effect as described in the preceding section. In that case molecular chains must be packed in such a manner that at least two different intermolecular environments surrounding the C1 and C4 carbons are defined. The effects of hydrogen bonding associated with O5 and O1 oxygens might be somewhat significant. These effects are very difficult to be precisely estimated at present. Nevertheless, it can be concluded here that the crystal structure of the group of valonia and bacterial celluloses are different from that of the group of cotton and ramie, although the same crystal structure of cellulose I has been assumed for all these samples in the *x*-ray crystal analyses.[22–25] This conclusion has been confirmed by our recent CP/MAS study[28,29] of the same celluloses in the presence of water, where the C1 and C4 lines split into triplet for all samples but the relative intensities are also different from each other group.

On the other hand, the results for regenerated cellulose are different from both groups of native cellulose; both C1 and C4 carbons split into two lines. This fact may be related to the crystal structure of cellulose II but the detailed structure must be also re-examined by considering two kinds of values for both ϕ and ψ or two different kinds of intermolecular environments for C1 and C4 carbons. In addition, the chemical shifts of the C6 carbon are 63.7–64.1 ppm for the regenerated cellulose, which correspond to the *gauche-trans* conformation as is seen in Fig. 9. This conflicts with the result of *x*-ray crystal analyses,[23,25] where both *gauche-trans* and *trans-gauche* are assumed. In an *x*-ray crystal refinement this fact must be also considered.

Table 3 shows that the noncrystalline components of native cellulose have no significant difference in chemical shift and linewidth from each other. The chemical shifts of the regenerated cellulose fibers are also almost the same as those of native cellulose. This may suggest that the most probable conformation of the regenerated fibers is very similar to that of native cellulose. However, there is a marked difference in line width $\Delta\nu$ of the C1 and C4 carbons between native and regenerated celluloses; the linewidth of the C1 carbon of native cellulose is about half that of the regenerated

cellulose. Although the cause of the line broadening in CP/MAS spectra is not clear as yet, it is most likely that the linewidths of the C1 and C4 carbons are primarily dependent on the distributions of the torsion angles ϕ and ψ. Thus, it is suggested that the distributions in the angles ϕ and ψ are relatively narrow for the noncrystalline component of native cellulose compared with those of regenerated cellulose. This means that the conformation of the noncrystalline component is comparatively confined for native cellulose, whereas in the regenerated cellulose fibers it is rather versatile. The result obtained here is in good accord with our previous ^{1}H broad-line NMR analyses[30,31] which indicate that the noncrystalline component of regenerated cellulose fibers is much enhanced in molecular mobility by such a swelling agent as DMSO, whereas no significant effect appears for native cellulose.

d. Effects of Water on the Solid Structure of Cellulose[32]

Since cellulosic materials are usually used or treated in the presence of water, studies of the solid-state structure of wet cellulose samples are also of a great importance. However, as water is easily removable from a conventional MAS rotor by high centrifugation, it has been difficult to investigate the dependences of the water content on the spectra or the spin relaxation phenomena and therefore only a few reports were published.[33–35] In order to perform CP/MAS ^{13}C NMR experiments without the loss of water, we have developed a new MAS rotor with an *O*-ring seal by modifying a bullet-type rotor as shown in Fig. 10.

Figure 11 shows 50 MHz CP/MAS ^{13}C NMR spectra of cotton cellulose with different water contents. Both crystalline and noncrystalline lines of C4 and C6 carbons narrow with increasing water content. Also fine splitting of the C1 resonance is more

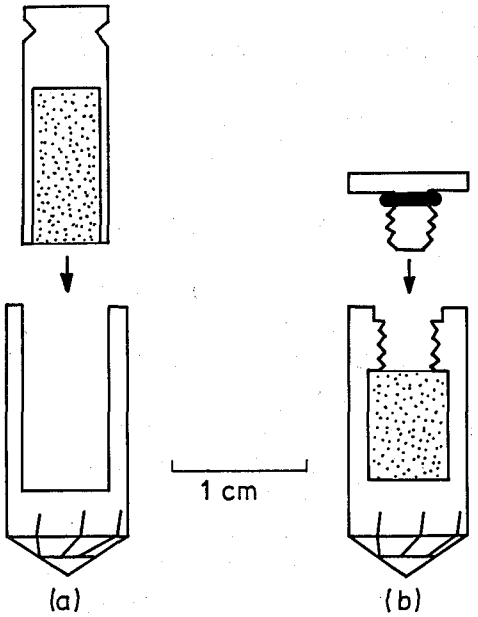

Fig. 10. Schematic diagrams of MAS rotors. (a) a conventional rotor; (b) a newly developed rotor with an *O*-ring seal.

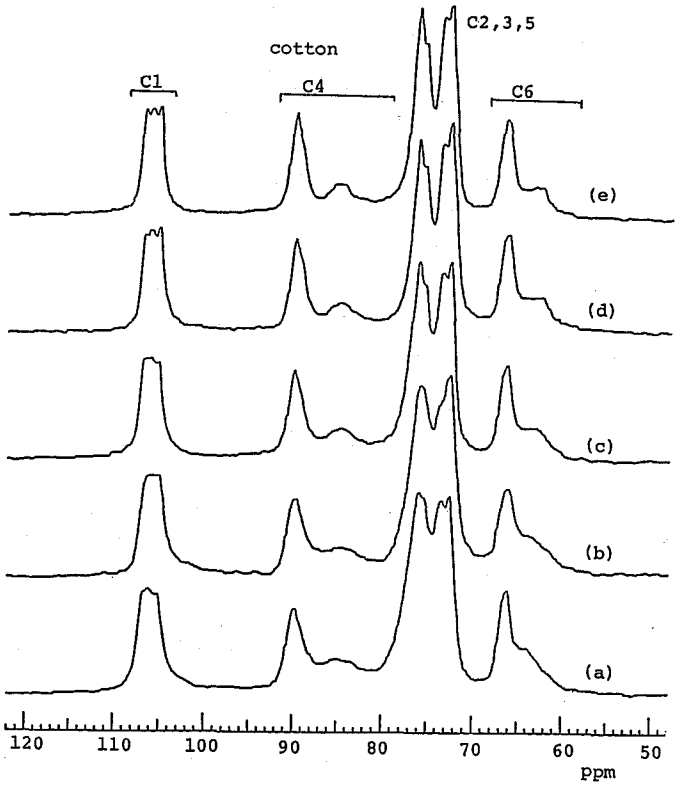

Fig. 11. 50 MHz CP/MAS ^{13}C NMR spectra of cotton cellulose with different water contents. (a) 0%; (b) 4.2%; (c) 8.4%; (d) 19.1% (e) 161%.

clearly observed. The noncrystalline resonance of the C6 carbon observed as an upfield shoulder seems to shift upfield with the increase of water content.

Figure 12 shows the CP/MAS ^{13}C NMR spectra of cupra rayon with different water contents. The line shapes of the respective resonances are quite different from those of cotton cellulose shown in Fig. 11. This is mainly due to the differences in crystal structure and crystallinity of these two samples. However, the influences of water content of the spectra of the rayon are very similar to the case of cotton cellulose. The doublets of the C1 and C4 lines ascribed to the crystalline component are more clearly observed for the samples with higher water contents. In the C6 resonance the splitting into the crystalline and noncrystalline components is enhanced by water as a result of the upfield shift of the broader noncrystalline component.

In order to further investigate the effects of water on the respective components, we have recorded the spectra of the crystalline and noncrystalline components in a similar way to that for the dry samples as shown in Fig. 5. Figure 13 shows the spectra of the crystalline components of cotton cellulose with the water contents of 0% and 161%. These spectra were obtained from the difference between the crystalline and noncrystalline components of ^{13}C T_1. The multiplicity of the C1 resonance is clearly seen in these spectra: in the dry state two nonequivalent lines constitute this resonance but they split into one doublet and one singlet in the hydrated state.

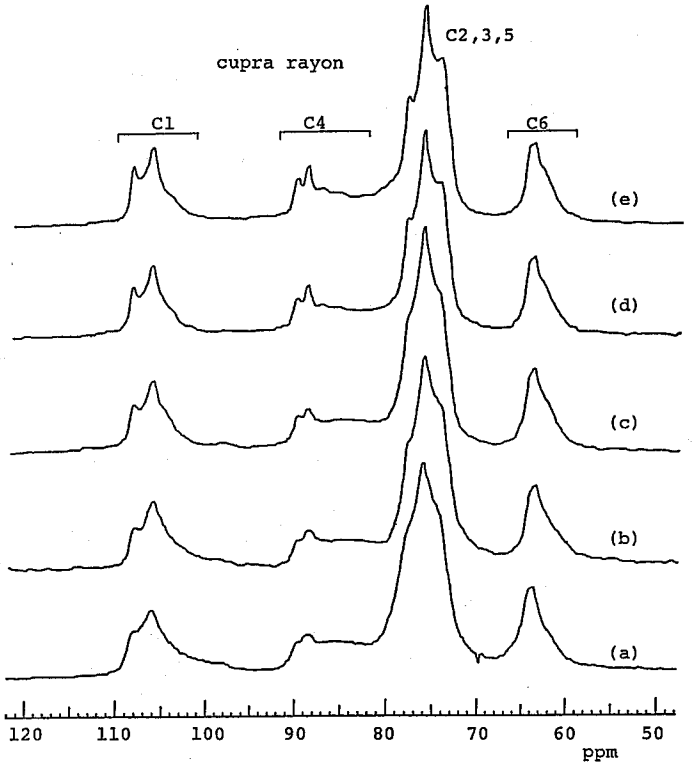

Fig. 12. 50 MHz CP/MAS ^{13}C NMR spectra of cupra rayon with different water contents. (a) 0%; (b) 7.6%; (c) 14.4%; (d) 36.4%; (e) 158%.

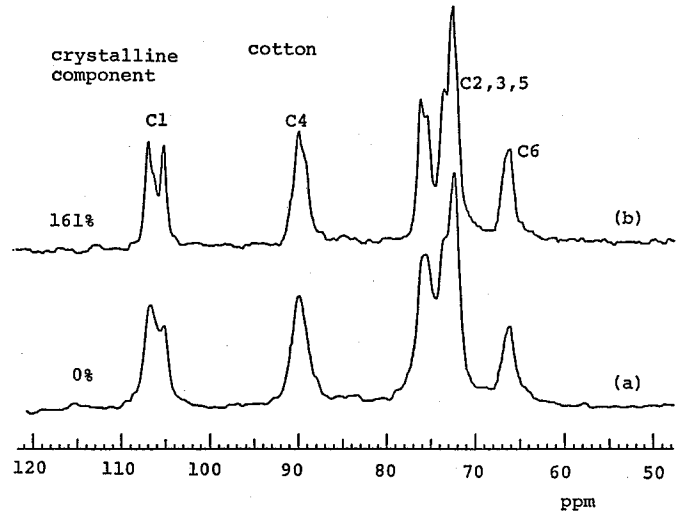

Fig. 13. CP/MAS ^{13}C NMR spectra of the crystalline components of cotton cellulose with the water contents of 0% (a) and 161% (b).

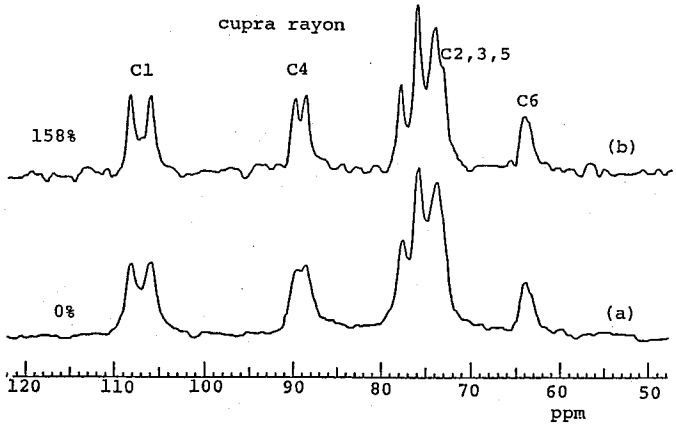

Fig. 14. CP/MAS ^{13}C NMR spectra of the crystalline components of cupra rayon with the water contents of 0% (a) and 158% (b).

Figure 14 shows the spectra of the crystalline components obtained from the cupra rayon with the water contents of 0% and 158%. It is clearly seen that water significantly narrows each resonance, although the features of each line remain unchanged. The resonance lines of the crystalline component of native and regenerated samples narrow but the chemical shifts remain constant. Therefore, it is likely that water does not greatly affect the crystal structures of Cellulose I and Cellulose II (defined for native and regenerated celluloses, respectively). However, since most of the crystalline lines become narrower and split more clearly into multiple sublines, it is suggested that some distortion may be produced in the crystal lattice upon drying but it may be gradually relaxed with the increase of water content.

Figure 15 shows the spectra of the noncrystalline components of cotton cellulose with water contents of 0% and 161%. These spectra were obtained by subtracting

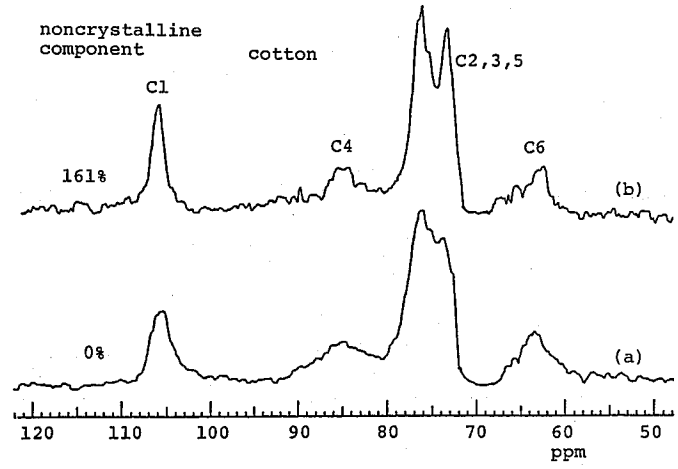

Fig. 15. CP/MAS ^{13}C NMR spectra of the noncrystalline components of cotton cellulose with the water contents of 0% (a) and 161% (b).

the spectra of the crystalline components in Fig. 13 from the corresponding whole spectra shown in Fig. 11a and 11e. In addition, such subtractions were made for the respective resonance lines since the intensities of the lines in the spectra of the crystalline components appreciably differ from each other owing to the differences in T_1. It is clearly seen that the linewidths of the C1 and C4 resonances become markedly narrower upon absorbing water, while holding the average chemical shifts unchanged.

Figure 16 shows the spectra of the noncrystalline components of cupra rayon with the water contents of 0% and 158%, which were obtained by the respective subtraction of their crystalline components (Fig. 14) from the corresponding whole spectra (Figs. 12a and 12e). In comparison with the case of cotton cellulose, the linewidths of the respective resonances do not remarkably decrease by the addition of water: for example, the half-value width of the C1 resonance line is 205 Hz for the hydrated sample, whereas it is 256 Hz for the dry sample. This fact indicates that the molecular mobility of the noncrystalline chains does not greatly increase with the increase of water content. Since the molecular conformation of this component is rather relaxed even in the dry state, no appreciable change occurs in its conformation on the water sorption. On the other hand, in the case of cotton it is concluded that water does not significantly enhance the segmental motion but relaxes the noncrystalline chain from a distorted state to a relatively ordered state.

Figure 17 shows the schematic structural models of native and regenerated cellulose samples. The native cellulose after biosynthesis is supposed to crystallize from the ordered state such as liquid state. Hence the noncrystalline component seems to be in the relatively ordered state. The chains may undergo some distorsion upon drying, but on the water sorption such a distorsion may be relaxed. As a result resonance lines of cotton become narrow as shown in Fig. 14.

On the other hand, the regenerated cellulose fibers are produced by spinning from the concentrated solution in which molecular chains are coiled and entangled with each other. Therefore it is thought that the noncrystalline chains in the regenerated cellulose fibers are rather random. Such relaxed chains may hardly undergo marked

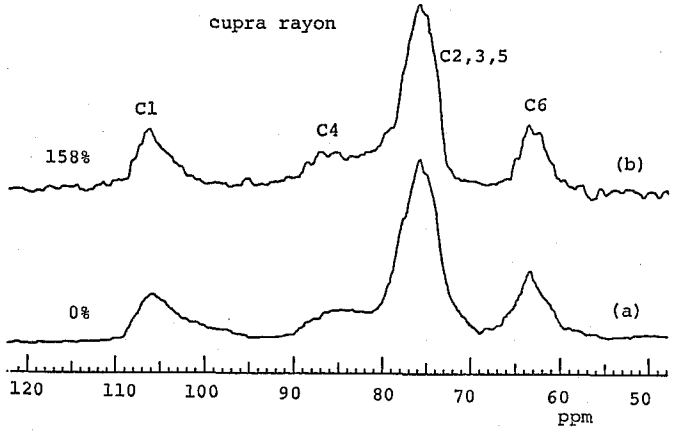

Fig. 16. CP/MAS ^{13}C NMR spectra of the noncrystalline components of cupra rayon with the water contents of 0% (a) and 158% (b).

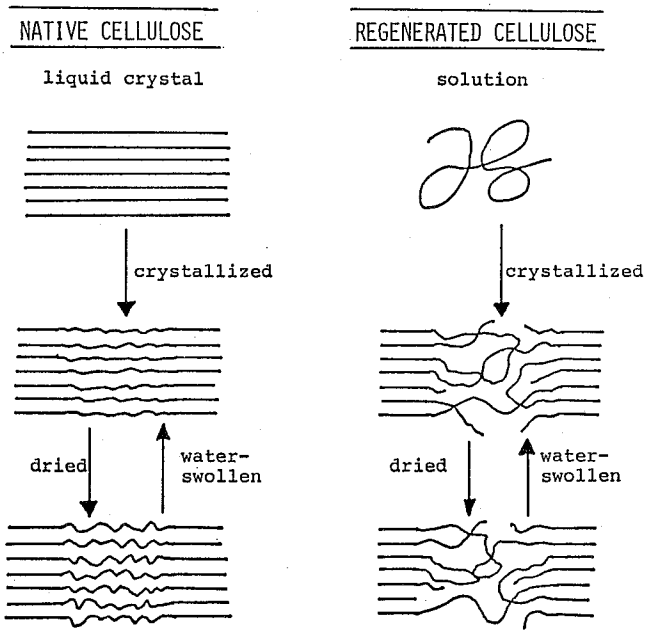

Fig. 17. Schematic structural models of native and regenerated cellulose samples.

distortion upon drying and large change in conformation upon absorbing water. This feature of the noncrystalline chains of cupra rayon must be reflected on the insignificant decrease in the resonance lines of the hydrated sample.

REFERENCES

(1) D. L. VanderHart, *Macromolecules*, **12**, 1232 (1979).
(2) F. Horii, R. Kitamaru, S. Maeda, A. Saika and T. Terao, *Polym. Bull.*, **13**, 179 (1985).
(3) D. L. VanderHart, G. G. A. Bohm and V. D. Mochel, *ACS Polym. Prepr.*, **22**, 261 (1981).
(4) See, for example, R. Kitamaru, C-13 Nuclear Spin Relaxation in "Stereochemical Applications of NMR Spectroscopy", Y. Takeuchi and P. Marchand, Eds., Verlag Chemie International, 1985.
(5) F. Horii, A. Hirai and R. Kitamaru, *J. Carbohydr. Chem.*, **3**, 641 (1984).
(6) F. Horii, A. Hirai and R. Kitamaru, *ACS Symposium Series*, **260**, 28 (1983).
(7) J. C. Gast, R. H. Atalla and R. D. McKelvey, *Carbohydr. Res.*, **84**, 137 (1980).
(8) R. H. Atalla, J. C. Gast, D. E. Sindorf, V. J. Bartuska and G. E. Maciel, *J. Am. Chem. Soc.*, **102**, 3249 (1980).
(9) W. L. Earl and D. L. VanderHart, *J. Am. Chem. Soc.*, **102**, 3251 (1980).
(10) F. Horii, A. Hirai and R. Kitamaru, *Polym. Bull.*, **8**, 163 (1982).
(11) D. A. Torchia. *J. Magn. Reson.*, **30**, 613 (1978).
(12) D. L. VanderHart, *J. Magn. Reson.*, **44**, 117 (1981).
(13) F. Imashiro, S. Maeda, K. Takegoshi, T. Terao and A. Saika, *Chem. Phys. Lett.*, **92**, 642 (1982); **99**, 189 (1983).
(14) T. Terao, S. Maeda and S. Saika, *Macromolecules*, **16**, 1535 (1983).
(15) P. E. Pfeffer, K. M. Valentine and F. W. Parrish, *J. Am. Chem. Soc.*, **101**, 1265 (1979).
(16) P. E. Pfeffer, K. B. Hicks, M. H. Frey and S. J. Opella, *J. Carbohydr. Chem.*, **3**, 197 (1984).
(17) S. S. C. Chu and G. A. Jeffrey, *Acta Cryst.*, **B24**, 830 (1968).
(18) D. C. Fries, S. T. Rao and M. Sundaralingam, *Acta Cryst.*, **B27**, 994 (1971).
(19) K. Hirotsu and A. Shimada, *Bull. Chem. Soc. Japan*, **47**, 1872 (1974).
(20) C. J. Brown, *J. Chem. Soc.*, (A), 927 (1966).

(21) J. T. Ham and D. G. Williams, *Acta Cryst.*, **B26**, 1373 (1970).
(22) K. H. Gardner and J. Blackwell, *Biopolymers*, **13**, 1975 (1974).
(23) K. J. Kolpak and J. Blackwell, *Macromolecules*, **9**, 273 (1976).
(24) C. Woodcock and A. Sarko, *Macromolecules*, **13**, 1183 (1980).
(25) A. J. Stipanovic and A. Sarko, *Macromolecules*, **9**, 851 (1976).
(26) S. Perez, J. S.-Pierre and R. H. Marchessault, *Can. J. Chem.*, **56**, 2866 (1978).
(27) F. Horii, A. Hirai and R. Kitamaru, *Polym. Bull.*, **10**, 357 (1983).
(28) A. Hirai, F. Horii and R. Kitamaru, *Polym. Prepr., Japan*, **34**, No. 9, 2473 (1985).
(29) F. Horii, A. Hirai and R. Kitamaru, *Annual. Report of the Research Institute for Chemical Fibers, Japan*, **42**, 41 (1985).
(30) A. Hirai, F. Horii and R. Kitamaru, *J. Polym. Sci. Polym. Phys. Ed.*, **18**, 1801 (1980).
(31) A. Hirai, R. Kitamaru, F. Horii and I. Sakurada, *Cellulose Chem. Technol.*, **14**, 611 (1980).
(32) F. Horii, A. Hirai, R. Kitamaru and I. Sakurada, *Cellulose Chem. Technol.*, **19**, 513 (1985).
(33) D. L. VanderHart, *NBS Report* NMAIR 82-2534 (1982).
(34) D. L. VanderHart and R. H. Atalla, *Macromolecules*, **17**, 1465 (1984).
(35) C. A. Fyfe, P. J. Stephenson, H. G. Taylor, T. L. Bluhm, Y. Deslandes and R. H. Marchessault, *Macromolecules*, **17**, 501 (1984).